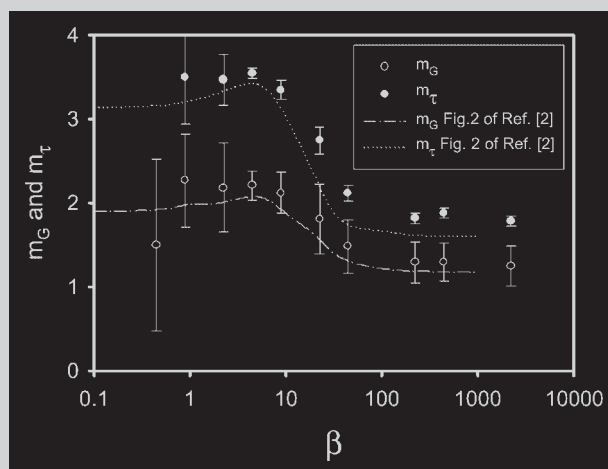


**Summary:** Polymer orientation in dilute solutions undergoing shear flow is investigated computationally by means of the Brownian dynamics simulation technique applied to the bead-spring chain model. The dependence of the degree of orientation on the shear intensity is evaluated through a quantity called orientation resistance. All simulations were performed using non-preaveraged hydrodynamic interaction (HI). The spring type (Gaussian or FENE) is shown to strongly determine the shear flow behavior of the chain orientation. Solvent quality ( $\Theta$ , good or bad), represented by a suitable Lennard-Jones intramolecular potential, does not affect the flow behavior but influences the values of the orientation resistance. Hence, the orientability of the polymer molecule is, in a way, related to the flow intensity.



Evolution of  $m_G$  (orientational resistance parameter, open circles are simulation, dashed line is Gaussian approximation) and  $m_\tau$  (filled circles are simulation, dotted line is Gaussian approximation) with  $\beta$  for ideal Gaussian chains with  $N = 15$ .

## Orientation of Polymer Chains in Dilute Solution under Shear: Effect of Chain Model and Excluded Volume

José G. Hernández Cifre,\* José García de la Torre

Departamento de Química Física, Facultad de Química Universidad de Murcia, 30071 Murcia, Spain

Fax: (+34) 968 364148; E-mail: jghc@um.es

Received: October 3, 2003; Revised: December 23, 2003; Accepted: January 7, 2004; DOI: 10.1002/mats.200300023

**Keywords:** bead-spring; dilute solution; excluded volume; orientation; simulations

### Introduction

Theoretical and computational studies of the rheological properties of polymeric systems require the formulation of adequate models. A classical coarse-grained representation of flexible polymer chains, which ignores unnecessary chemical details but still captures features relevant to rheological purposes, is the bead-and-spring model.<sup>[1]</sup> In this model, the elements are spheres which experience some friction in the viscous solvent, and the connectors are springs which represent the variability of distances between parts of the polymer chain. Even for such simplified models, a fully theoretical treatment is usually very difficult or even impossible. Then, one has the recourse of performing computer simulations of the behavior of the

system. The dynamics of polymers in dilute solution are dominated by the Brownian motion of the chain elements in the viscous flow, and the hydrodynamic and energetic interactions between them. For these cases, the proper simulation technique is Brownian dynamics (BD) simulation.

It is well known that flexible polymer molecules in dilute solution are deformed and oriented by flow. A way of characterizing the orientation phenomena is by using optical techniques, such as those of flow birefringence and radiation scattering. Through these experimental techniques the so-called orientation angle, giving the degree of alignment of the polymer with the flow, and the closely related orientation resistance parameter can be obtained. However, these measurement techniques give rise to different results due to the different length scales and tensorial quantities

involved.<sup>[2]</sup> Hydrodynamic and thermodynamic (solvent power) effects coming from the solvent, as well as the polydispersity of the sample, significantly influence the orientational process. To account for these factors in theory and simulation studies we must add influences coming from the chain model used to represent and solve the polymer dynamics. In this work we will show the influence of the chain model and the solvent quality on the orientational behavior of a polymer coil that experiences a simple shear flow by computationally reproducing the results that would be obtained for the orientation resistance parameter by the application of the two above mentioned experimental techniques.

## Theory and Methodology

### Theoretical Background

We consider the simple and usual case in which a dilute polymer solution is subjected to a simple shear flow. The flow velocity is along direction  $x$  and the shear plane is  $(x, y)$ . The velocity profile is therefore given by Equation (1).

$$v_x = \dot{\gamma}y \quad v_y = 0. \quad v_z = 0, \quad (1)$$

where  $\dot{\gamma}$  is the shear rate, the only nonzero component of the velocity gradient tensor. It is customary to express the shear rate in a dimensionless way by multiplying it by a characteristic relaxation time of the polymer [Equation (2)].

$$\beta = \frac{M\eta_s[\eta]_0}{N_A k_B T} \dot{\gamma}, \quad (2)$$

where  $M$  is the polymer molecular weight,  $\eta_s$  is the solvent viscosity,  $[\eta]_0$  is the polymer zero-shear intrinsic viscosity,  $N_A$  is Avogadro's number,  $k_B$  is the Boltzmann constant and  $T$  is the absolute temperature.

When the magnitude of the shear rate exceeds the inverse of the characteristic time defined in Equation (2) (factor in front of  $\dot{\gamma}$ ), that is,  $\beta \geq 1$ , the chain becomes appreciably deformed and oriented along the flow direction, thus leaving the equilibrium random coil conformation and acquiring an overall elliptical symmetry. The orientation is quantified by the orientation angle,  $\chi$ , subtended by the major axis of an ellipsoid representing the overall statistical polymer conformation and the flow direction. Therefore,  $\chi$  decreases when the flow intensity increases. The axes of the ellipsoid correspond to the main directions of some characteristic tensorial property of the polymer. Because not all tensorial quantities have the same principal axes, the value of the orientational angle will depend on the tensor used for its definition and, therefore, on the experimental technique employed to measure it since each technique is related to different tensorial properties. Two techniques often used to study the orientational behavior of polymer molecules are flow birefringence and light scattering. The former is related to the stress tensor,  $\tau$ , whereas the latter is related

to the gyration tensor,  $G$ . Thus, orientation angles obtained by these techniques,  $\chi_\tau$  and  $\chi_G$  respectively, cannot be directly compared. In any case, it is possible to write down an equation relating the orientation angle to the components of the corresponding tensor [Equation (3)]<sup>[2]</sup>

$$\tan 2\chi_\tau = \frac{2\tau_{xy}}{\tau_{xx} - \tau_{yy}} = \frac{m_\tau(\beta)}{\beta} \quad (3)$$

and Equation (4):

$$\tan 2\chi_G = \frac{2G_{xy}}{G_{xx} - G_{yy}} = \frac{m_G(\beta)}{\beta}. \quad (4)$$

In Equation (3) and (4), the quantity  $m_i(\beta)$  ( $i = \tau, G$ ) is the so-called orientational resistance parameter the value of which depends on the dimensionless shear rate,  $\beta$ , and on the components of the tensor entering in the determination of the orientation angle. At small enough shear rates,  $\tau_{xy}$  is proportional to  $\beta$  and  $(\tau_{xx} - \tau_{yy})$  is proportional to  $\beta^2$ . Therefore, when  $\beta \rightarrow 0$  the orientation resistance must tend to some nonvanishing zero-shear-rate limit,  $m_i^0$  ( $i = \tau, G$ ), and the orientation angle  $\chi_i$  to  $45^\circ$ .

### Model and Simulation Procedure

A single linear flexible polymer is represented using the well-known bead-spring model<sup>[1,3]</sup> consisting of  $N$  beads connected linearly by  $N - 1$  Hookean or FENE (finite extensible nonlinear elongational) springs. Hookean springs are ruled by the linear law [Equation (5)].

$$\mathbf{F}_s = \frac{3k_B T}{b^2} \mathbf{Q}, \quad (5)$$

whereas the FENE force law is given by the expression [Equation (6)].<sup>[3]</sup>

$$\mathbf{F}_s = \frac{3k_B T}{b^2} \frac{\mathbf{Q}}{1 - (Q/Q_{\max})^2}. \quad (6)$$

In Equation (5) and (6),  $k_B T$  is the Boltzmann factor,  $\mathbf{Q}$  is the instantaneous spring vector,  $Q$  is its modulus and  $b$  determines the Hookean spring constant,  $H = 3k_B T/b^2$ . The parameter  $Q_{\max}$  in Equation (6) is the maximum allowed FENE spring extension, which in this work is set to  $Q_{\max} = 10b$ . The equilibrium conformational statistics of the flexible polymer chains are well represented by using both Hookean (Gaussian) and FENE springs. Nevertheless, at high shear rates, the more physically correct FENE model is necessary to account for the finite extensibility of the chains and is therefore more relevant for explaining the experimental data.

The thermodynamic polymer-solvent interaction is taken into account by defining intramolecular potentials between the polymer beads. We modeled the so-called excluded volume effect (EV), related to the impossibility of overlap of the different chain portions, using a Lennard-Jones (LJ)

potential.<sup>[4]</sup> The force between beads derived from this potential is [Equation (7)]:

$$\mathbf{F}_{LJ} = \frac{24\varepsilon_{LJ}}{r_{ij}^2} \left[ 2 \left( \frac{\sigma_{LJ}}{r_{ij}} \right)^{12} - \left( \frac{\sigma_{LJ}}{r_{ij}} \right)^6 \right] \mathbf{r}_{ij}, \quad (7)$$

where  $r_{ij}$  is the distance between beads  $i$  and  $j$  and  $\varepsilon_{LJ}$  and  $\sigma_{LJ}$  are the Lennard-Jones parameters. The former represents the energy minimum and the latter the distance at which the energy becomes zero. The quality of the solvent is modeled by assigning suitable values to these parameters. In the limit of very good solvents (EV conditions), the Lennard-Jones parameters are given by  $\sigma_{LJ} = 0.8b$  and  $\varepsilon_{LJ} = 0.1k_B T$ .<sup>[5]</sup> A  $\Theta$  solvent is represented by setting  $\varepsilon_{LJ} = 0.3k_B T$ <sup>[4]</sup> and bad solvents by setting  $\varepsilon_{LJ} > 0.3k_B T$ .<sup>[6]</sup> Some results are also obtained in the absence of any intramolecular potential (ideal conditions) which gives rise to the so-called phantom chain. This chain model reproduced the conformational statistic of the chains in the  $\Theta$  state quite well and is often used due to its simplicity.

The solvent is treated as a continuum in which the chain is embedded. Its effect is taken into account basically through the friction coefficient of the beads,  $\zeta_i = 6\pi\eta_s a$ , where  $\eta_s$  is the solvent viscosity and  $a = 0.247b$  is the hydrodynamic radius of the (identical) beads. A proper description of the polymer dynamics in dilute solution requires consideration of the solvent-mediated hydrodynamic interactions between beads, which are represented without pre-averaging approaches by using the Rotne-Prager-Yamakawa (or modified Oseen) tensor.<sup>[9,10]</sup> Previous work, including some from our group,<sup>[11]</sup> corroborates the importance of considering HI effects to obtain results comparable to experiments. The stochastic differential equation governing the dynamics of the polymer chain is integrated numerically over a small, finite time step,  $\Delta t$ , using the BD algorithm of Ermak and McCammon<sup>[7]</sup> with the predictor-corrector improvement of Iniesta and García de la Torre.<sup>[8]</sup>

## Results and Discussion

In this work we discuss the influence of the different kind of bonded (springs) and nonbonded (EV) interactions used to build the chain model on the orientational behavior of a single polymer molecule under shear flow. For all the cases simulated we took into account the HI effect as specified in the theoretical section.

Figure 1 shows in a semi-log plot the shear rate dependence of  $m_G$  and  $m_\tau$  for an ideal Gaussian chain of  $N = 15$  with HI as obtained from our simulations (circles) together with the corresponding values from Figure 2 in reference [2] (lines). In that figure, Bossart and Öttinger used the same chain model (bead-spring model,  $N = 15$ , no-EV, HI) to calculate analytically, by means of the Gaussian approximation, the dependence of the resistance parameter on  $\beta$ . It can be appreciated in Figure 1 that the values of both  $m_G$  and

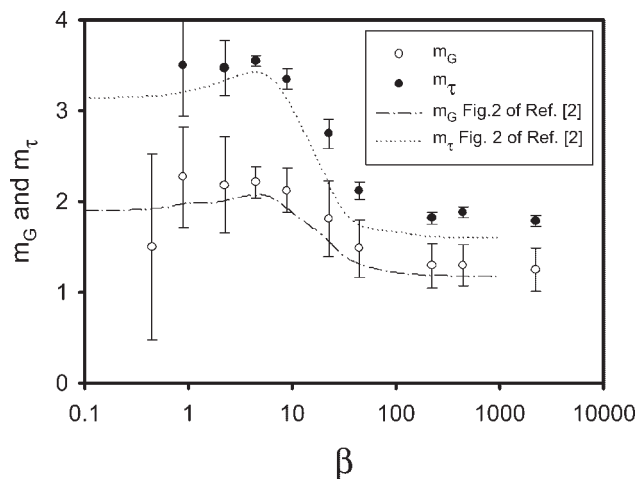


Figure 1. Evolution of  $m_G$  (open circles are simulation, dashed line is Gaussian approximation) and  $m_\tau$  (black circles are simulation, dotted line is Gaussian approximation) with  $\beta$  for ideal Gaussian chains with  $N = 15$ .

$m_\tau$  and their shear dependence compare quite well with the results from reference [2]. The values of Bossart and Öttinger are slightly smaller than the simulation results because, for the analytical approach,  $N = 15$  is a short chain and values of the orientation resistance (for a given hydrodynamic radius  $a$ ) increase with  $N$  up to reaching the limit for infinitely long chains, as shown in reference [2]. However, it seems that for this simulation technique, that number of beads is already large enough to give long-chain results. As also stated in reference [2] the deviation of the orientation resistance from its limiting  $N \rightarrow \infty$  value depends on the choice of the parameter  $a$ , but our choice is the same as that of Figure 2 in reference [2]. The first feature to note in Figure 1 is that  $m_\tau > m_G$  for every  $\beta$ , which will be true regardless of the chain model used. It means that, under the same flow conditions, the value of

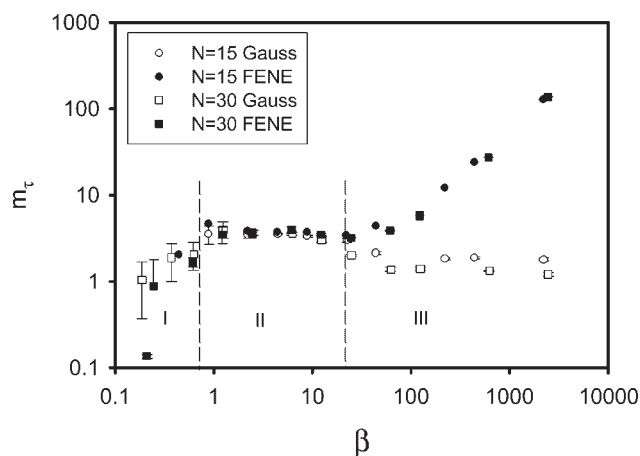


Figure 2. Influence of spring type. Evolution of  $m_\tau$  with  $\beta$  for ideal Gaussian chains (open symbols) and ideal FENE chains (black symbols) with  $N = 15$  (circles) and  $N = 30$  (squares).

the orientation angle measured by flow birefringence will be greater than that measured by radiation scattering techniques. In general terms, it can be appreciated that at relatively low shear rates (approximately  $1 < \beta < 8$ ), the orientation resistance stays approximately constant or increases slightly. Results at smaller shear rates present large error bars and, as we will comment later, a change on the  $\beta$  dependence of the orientation resistance seems to appear. Then, at intermediate shear rates, the orientation resistance diminishes quite strongly, the decay being steeper for  $m_\tau$  than for  $m_G$ , and at high shear rates it turns to reach a plateau. Thus, for the Gaussian model, orientation of polymer chains along the flow direction becomes easier with flow. As we show in brief, this result is not realistic and when using FENE springs that account for the finite extensibility of the polymer chain, the resistance to the orientation of the polymer increases strongly from a certain critical value of  $\beta$ .

Table 1 in reference [2] contains the limiting zero-shear-rate values of the resistance parameters (e.g.  $m_\tau^0$ ,  $m_G^0$ ) as calculated analytically by different approaches in the limit of  $N \rightarrow \infty$ . Among them, we find the values obtained from the Rouse model (no HI),  $m_\tau^0 = 2.50$ ,  $m_G^0 = 1.75$ , and the Zimm model (preaveraged HI),  $m_\tau^0 = 4.83$ ,  $m_G^0 = 2.55$ . The values obtained in our simulations assuming, as in theoretical approaches, the constancy of the orientation resistance for the whole low  $\beta$  range (i.e. the plateau reached around  $\beta = 1$  can be extrapolated to smaller  $\beta$ ) are  $m_\tau^0 \approx 3.5$  and  $m_G^0 \approx 2.1$ . This is in perfect agreement with the values obtained by Bossart and Öttinger using the Gaussian approximation, namely  $m_\tau^0 \approx 3.57$  and  $m_G^0 \approx 2.00$ , as well as with previous Brownian simulation values coming from previous works of our group,  $m_\tau^0 \approx 3.4$ .<sup>[12]</sup> Moreover, a value of  $m_G^0 \approx 2.1$  was reported from light-scattering experiments of dilute solutions of polystyrene at  $\Theta$  conditions<sup>[13]</sup> and suggested was by nonequilibrium molecular dynamics simulations.<sup>[14]</sup>

Figure 2 shows, in a log-log plot, the greatly different flow behavior of  $m_\tau$  (analogously for  $m_G$ ) when using Gaussian or FENE springs. This figure contains results for ideal chains with both  $N = 15$  and  $N = 30$ . As expected, at a low shear rate  $\beta$  (below a certain critical value), there is almost no difference between FENE and Gaussian chain behavior. It can be appreciated, more clearly for FENE chains and  $N = 30$ , that three regions (roughly delimited by dashed lines) similar to those observed experimentally by Zisenis and Springer<sup>[15]</sup> seem to appear. At very low  $\beta$  (region I, onset of the orientation) orientation resistance rapidly increases with  $\beta$ , then, at intermediate shear rates (region II) it becomes approximately constant with a certain value  $m_\tau^0 \approx 3.4$ , as predicted by extrapolation in theoretical approaches, or increases very slightly. Finally, at high  $\beta$ ,  $m_\tau$  increases again strongly (FENE) or decreases (Gaussian) with  $\beta$ . Changes from one region to another occur at approximately the same  $\beta$  value, independent of

the chain length,  $N$ , since  $\beta$  makes the results independent of molecular weight as long as the shear rate is not so high that chains are appreciably deformed. In conclusion, from a critical  $\beta$  ( $\approx 20$  for ideal chains), the behavior of FENE chains increasingly diverges from that of Gaussian chains. As expected, the orientation of FENE chains becomes more difficult when increasing the shear rate because of the increasing difficulty in further extension of FENE springs. This increase of the orientation resistance with the shear rate is found in all simulations with FENE chains (see for example Aust et al.<sup>[16]</sup> where authors use nonequilibrium molecular dynamics technique instead of Brownian Dynamics) and also in experimental works.<sup>[13,15,17]</sup> Figure 3 shows a comparison of the behavior of the parameters  $m_G$  and  $m_\tau$  for a FENE ideal chain with  $N = 30$ . Again, the values of  $m_G$  are smaller than those of  $m_\tau$  for the whole  $\beta$  range. The positive slope of  $m_\tau$  at high  $\beta$  is slightly steeper than that of  $m_G$ , in a similar way to the steeper decay of  $m_\tau$  in the case of Gaussian chains.

Figure 4a (Gaussian) and 4b (FENE) show the effect of the inclusion of intramolecular LJ potential to represent excluded volume interactions on the variation of  $m_\tau$  with  $\beta$ . Both graphs correspond to chains with  $N = 30$ . As can be appreciated, the inclusion of the LJ potential has no influence on the qualitative flow behavior of the orientational process, but it certainly influences the values of the orientational resistance parameter. Furthermore, the effect of the solvent quality seems to be related to the shear rate intensity. The maximum difference in the orientation parameter values appears at intermediate shear rates ( $5 < \beta < 100$ ). First of all, it should be noted that ideal chains without intramolecular potential, present a much lower value of the orientation resistance because the bond crossing facilitates the orientational process. At low  $\beta$  ( $< 1$ ), more clearly appreciable for FENE chains, the orientation resistance seems to be (in spite of the large error bars) slightly lower

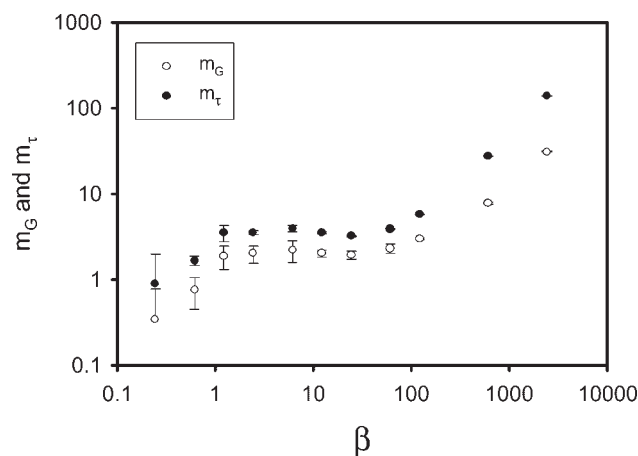


Figure 3. Comparison of the evolution of  $m_G$  (open circles) and  $m_\tau$  (black circles) with  $\beta$  for an ideal FENE chain with  $N = 30$ .

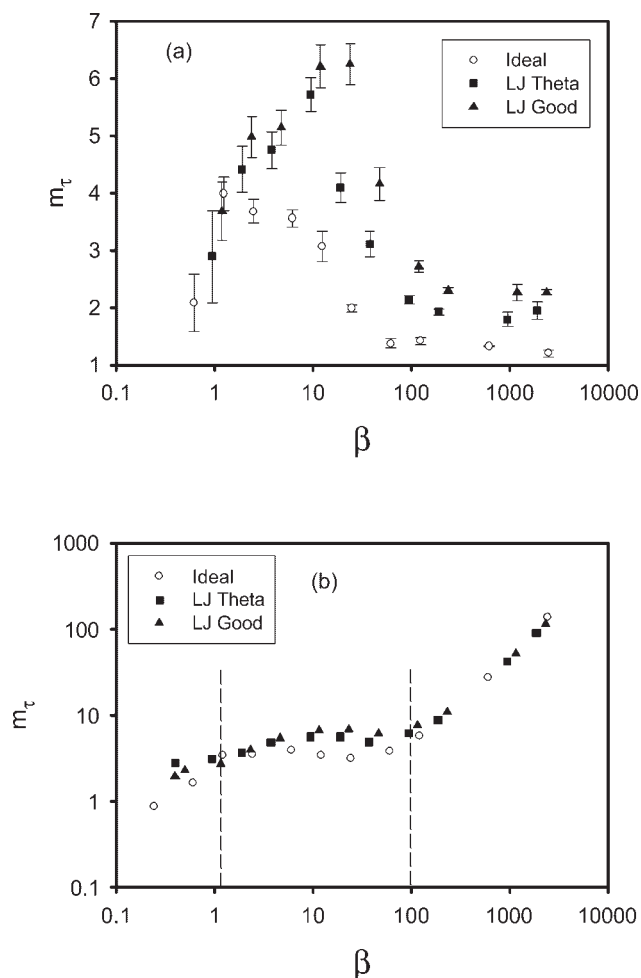


Figure 4. Influence of EV intramolecular interactions. Evolution of  $m_\tau$  with  $\beta$  for a) Gaussian and b) FENE chains with  $N=30$ . Ideal chain (open circles),  $\Theta$  solvent (black squares) and good solvent (black triangle).

for good solvent conditions than for  $\Theta$  solvent conditions. This is a type of behavior suggested by renormalization group calculations<sup>[18]</sup> and is found in some experiments.<sup>[15]</sup> However, at flow intensities so small there is no significant polymer orientation and therefore the effect of the solvent quality on the orientational parameters is not clear. At  $\beta$  around 1 there is a crossover, the solvent power influence becomes negligible, and an inversion of the above EV dependency occurs. Thus, orientation resistance starts to increase slightly with improving solvent power, that is, it is higher for good solvent conditions, both for Gaussian and FENE chains. At intermediate shear rates, the EV influence on the values of the orientation resistance is clear and much more significant for Gaussian than for FENE chains (Figure 4a and 4b must not be directly compared because of the linear versus log scale in  $m_\tau$  axis). Besides, Gaussian chains with LJ potential present a strong increase of the  $m_\tau$  values at intermediate  $\beta$  before the final decay. In the case of

FENE chains, the presence of the LJ potential increases the values of  $m_\tau$ , as expected, with respect to those of ideal chains, but in any case a plateau region before the sudden final positive slope is obtained. At high shear rates ( $\beta > 100$ ), chains are quite stretched on average and the intramolecular LJ potential that represents EV interactions plays a less significant role in the polymer dynamics. Therefore its influence starts to be less important than at intermediate shear rates, although an improvement of the solvent quality increases orientation resistance. As can be appreciated from Figure 4a, the excluded volume effect is much more remarkable when using Gaussian chains. Finally, it must be noticed that the critical  $\beta$  values for regime changes, both in Gaussian and FENE chains, are practically independent of solvent quality.

To make clearer the influence of the solvent quality on the orientation resistance under favorable orientational conditions, that is,  $\beta \gg 1$ , Figure 5a shows the values of  $m_\tau$  (analogous for  $m_G$ ) for a FENE chain with  $N=30$  at  $\beta = 10$  and  $\beta = 100$  versus different values of the LJ parameter  $\varepsilon_{LJ}$ , that is, different solvent qualities including bad solvent conditions (as indicated in the plot). The values  $\beta = 10$  and  $\beta = 100$  are adequate to obtain significant polymer orientation. The orientation resistance parameter diminishes as the solvent quality becomes poorer (increasing  $\varepsilon_{LJ}$ ). Thus, polymer molecules become more oriented with the flow direction as solvent quality decreases. These simulation results are in complete agreement with the experimental findings of Lee and Muller.<sup>[17]</sup> It can also be clearly observed that the difference between good and  $\Theta$  solvents is small, the polymer molecule being slightly less oriented in good solvents. This is again in agreement with Lee and Muller and also with the birefringence experiments of Bossart and Öttinger.<sup>[19]</sup> When the solvent starts to become very poor, differences in the orientation parameter again start to become negligible. Therefore at intermediate and high shear rates there seems to exist a maximum  $m_\tau$  for very good solvent and a gradual decrease in the orientation resistance is seen when the solvent quality gets worse. Note here that we are dealing with bad solvents for which polymer chains are not yet in the globular state. If the solvent is so bad that the chains become globular, the situation would change. As mentioned above, the behavior displayed at both  $\beta$  values is the same, but the decay in worsening solvent power is less steep at higher  $\beta$  because EV interactions are less abundant. However, as specified above, Figure 5a contradicts experiments by Zisenis and Springer<sup>[15,20]</sup> who found that the orientation resistance decreased with the quality of the solvent, as well as some theoretical predictions in the same sense.<sup>[2,18]</sup> Lee and Muller<sup>[17]</sup> also made the observation that their experimental results contradict those of Zisenis and Springer.<sup>[15,20]</sup> It must be noticed that most of the experimental and theoretical work compares good and  $\Theta$  solvent conditions at low shear rates. No consideration is made of bad solvents

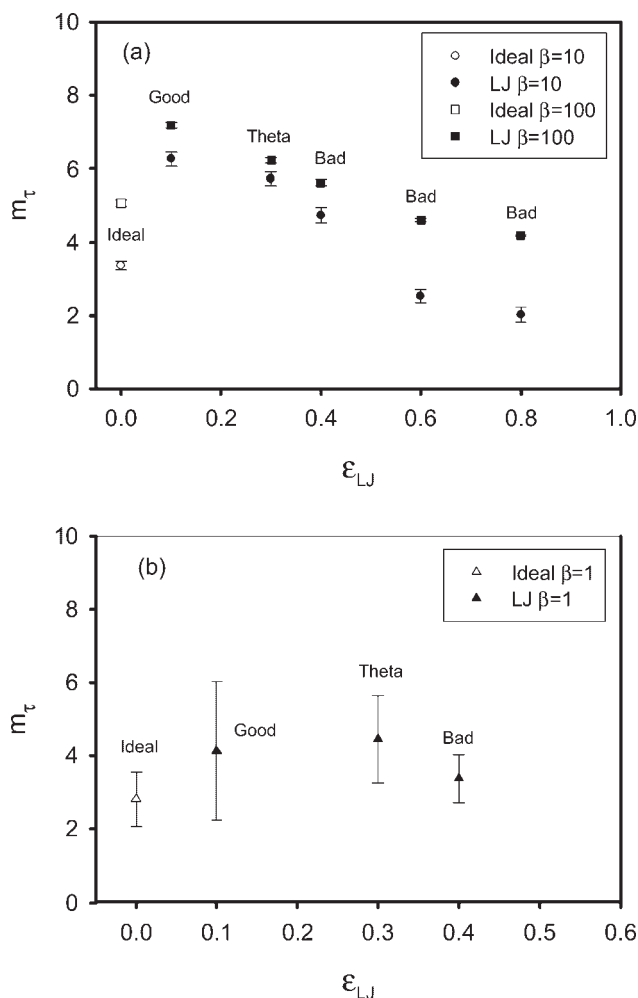


Figure 5. Influence of solvent quality. Dependence of  $m_\tau$  on the LJ parameter  $\epsilon_{LJ}=0$  (ideal), 0.1 (good), 0.3 ( $\Theta$ ), 0.6, 1.0 (bad) for a FENE chain with  $N=30$  at a)  $\beta=10$  and  $\beta=100$  and b)  $\beta=1$ .

and dimensionless shear rates greater than 10. Furthermore, as already stated, many of these works<sup>[2,18,19]</sup> find the excluded volume effect negligible. To clarify this point, Figure 5b shows simulation results for different solvent qualities at  $\beta=1$ , for which the polymer orientation is in any case small. Values for  $\epsilon_{LJ}>0.4$  are not shown because they present huge error bars and a globular conformation possibly starts to appear. As observed, solvent quality has little importance on the value of the orientation resistance, and, in spite of the large error bars, it seems that good solvent conditions slightly lower the value of  $m_\tau$ . In any case (Figure 5a and 5b), for ideal chains ( $\epsilon_{LJ}=0$ )  $m_\tau$  does not follow the trend and takes a very low value, that is, the phantom chain is more easily orientable. Most of the experimental works cited here employ the light scattering technique<sup>[13,15,17,20]</sup> which, as mentioned in the theoretical section, is related to  $m_G$  rather than to  $m_\tau$ . Nevertheless, the influence of solvent quality on  $m_G$  and  $m_\tau$  shear behavior is analogous.

## Conclusion

The Brownian dynamics simulation technique is an adequate tool for investigating the orientational behavior of polymer molecules in dilute solution which are subjected to shear flow. The values of the orientation resistance or, analogously, the orientation angle, that would be obtained by using flow birefringence and radiation scattering techniques can be obtained quite easily and used to determine the effect of the chain model parameters (spring and intramolecular forces) on the orientational behavior.

We have shown that the value and shear flow behavior of the orientation resistance parameter ( $m_\tau$  in case of flow birefringence measurements and  $m_G$  in case of light scattering measurements) depends strongly on the type of spring employed in the chain model, mainly at high  $\beta$ , when the orientation is precisely higher. Thus, orientation resistance becomes larger with flow intensity for FENE chains and smaller for the Gaussian model.

The use of intramolecular potentials to model the solvent quality, although of no influence on the qualitative orientational flow behavior, does influence to some extent the values of the orientation resistance and therefore the value of the orientation angle. There is some controversy in experimental works regarding the kind of influence of the solvent quality on the orientational process.<sup>[15,17]</sup> Simulations can help us to understand the solvent power effect and the cause of these discrepancies more fully. Thus, we obtain that at intermediate shear rates, where orientation is important and excluded volume effects play a principal role, the orientational process becomes more difficult with increasing solvent power. In this sense, simulations fully support the light scattering experiments of Lee and Muller.<sup>[17]</sup> Nevertheless there are not large differences in the values of the orientation resistance for good and  $\Theta$  solvent conditions and the intensity of the applied shear flow seems to affect their influence. Thus, in weak flows,  $\beta \leq 1$ , where the orientation phenomenon starts to appear, good solvent seems to help orientation with respect to  $\Theta$  solvent, but in flows where the chain is clearly oriented,  $\beta > 1$ , a good solvent makes orientation more difficult.

*Acknowledgements:* This work has been supported by grant BQU2003-04517 from *Dirección General de Investigación*, MCYT. J.G.H.C. is the recipient of a Ramón y Cajal postdoctoral research contract.

- [1] P. E. Rouse, *J. Chem. Phys.* **1953**, *21*, 1272.
- [2] J. Bossart, H. C. Öttinger, *Macromolecules* **1995**, *28*, 5852.
- [3] R. B. Bird, C. F. Curtiss, R. C. Armstrong, O. Hassager, "Dynamics of Polymeric Liquids, Kinetic Theory", Vol. 2, 2nd edition, Wiley, New York 1987.
- [4] J. J. Freire, A. Rey, J. García de la Torre, *Macromolecules* **1986**, *19*, 457.

- [5] A. Rey, J. J. Freire, J. García de la Torre, *Macromolecules* **1987**, *20*, 342.
- [6] A. Rey, J. J. Freire, J. García de la Torre, *Macromolecules* **1987**, *20*, 2386.
- [7] D. L. Ermak, J. A. McCammon, *J. Chem. Phys.* **1978**, *69*, 1352.
- [8] A. Iniesta, J. García de la Torre, *J. Chem. Phys.* **1990**, *92*, 2015.
- [9] J. Rotne, S. Prager, *J. Chem. Phys.* **1969**, *50*, 4831.
- [10] H. Yamakawa, *J. Chem. Phys.* **1970**, *53*, 436.
- [11] J. G. Hernández Cifre, J. García de la Torre, *J. Rheol.* **1999**, *43*, 339.
- [12] K. D. Knudsen, A. Elgsaeter, J. J. López Cascales, J. García de la Torre, *Macromolecules* **1993**, *26*, 3851.
- [13] A. Link, J. Springer, *Macromolecules* **1993**, *26*, 464.
- [14] C. Pierleoni, J.-P. Ryckaert, *Macromolecules* **1995**, *28*, 5097.
- [15] M. Zisenis, J. Springer, *Polymer* **1995**, *36*, 3459.
- [16] C. Aust, M. Kröger, S. Hess, *Macromolecules* **1999**, *32*, 5660.
- [17] E. C. Lee, S. J. Muller, *Polymer* **1999**, *40*, 2501.
- [18] H. C. Öttinger, *Phys. Rev. A* **1989**, *40*, 2664.
- [19] J. Bossart, H. C. Öttinger, *Macromolecules* **1997**, *30*, 5527.
- [20] A. Link, M. Zisenis, B. Protzl, J. Springer, *Makromol. Chem. Macromol. Symp.* **1992**, *61*, 358.